How to cite: *Angew. Chem. Int. Ed.* **2022,** *61,* e202201093
International Edition: doi.org/10.1002/anie.202201093
German Edition: doi.org/10.1002/ange.202201093

Surface Coating Hot Paper

N-Heterocyclic Carbene Based Nanolayer for Copper Film Oxidation Mitigation

Iris Berg[+]*, Einav Amit*[+]*, Lillian Hale, F. Dean Toste, and Elad Gross**

Abstract: The wide use of copper is limited by its rapid oxidation. Main oxidation mitigation approaches involve alloying or surface passivation technologies. However, surface alloying often modifies the physical properties of copper, while surface passivation is characterized by limited thermal and chemical stability. Herein, we demonstrate an electrochemical approach for surface-anchoring of an *N*-heterocyclic carbene (NHC) nanolayer on a copper electrode by electro-deposition of alkyne-functionalized imidazolium cations. Water reduction reaction generated a high concentration of hydroxide ions that induced deprotonation of imidazolium cations and self-assembly of NHCs on the copper electrode. In addition, alkyne group deprotonation enabled on-surface polymerization by coupling surface-anchored and solvated NHCs, which resulted in a 2 nm thick NHC-nanolayer. Copper film coated with a NHC-nanolayer demonstrated high oxidation resistance at elevated temperatures and under alkaline conditions.

Introduction

Copper is widely used in the electronic industry due to its high conductivity, ductility, and low price.[1] However, the integration of copper in cutting-edge applications, such as printed electronics,[2] is limited by its high susceptibility to corrosion, which degrades the electrical and mechanical properties of the metal.[3] Unlike other metals such as aluminum, the oxide layer on copper is not self-protecting and can continuously grow and deteriorate the conductivity and ductility of the metal.[3a] In addition, the kinetics of copper oxidation are rapid and an oxide layer is formed on the metal even under ambient conditions.[4] Therefore, there is a continuous search towards the development of new approaches to prevent or hinder copper oxidation.[5]

Efforts for copper oxidation mitigation can be divided into two main approaches. Copper oxidation can be inhibited by alloying with other metals, e.g., Al, Be, and Mg.[3a,6] However, alloying is not necessarily limited to the copper surface, and can impact the bulk properties of copper films.[5] A different approach is based on passivation of the copper surface with inorganic[7] or organic[5,8] monolayers. The main advantage of this approach is that the protective monolayers do not modify the bulk properties of copper. However, it should be noted that monolayers on copper films were characterized by a limited chemical and thermal stability.[8a,9] In addition, protection by monolayers was found less effective on corrugated surfaces or surfaces with a high density of defects, in which monolayers do not provide optimal coverage.[5,8a,10]

Multilayer formation can therefore offer improved protection against surface oxidation. Azole and benzotriazole compounds were used as precursors for multilayer formation on copper films for oxidation mitigation.[11] The unsaturated nitrogen atoms in benzotriazole function as surface-anchoring points,[11b,12] and benzotriazole complexation with Cu^{I} enabled the formation of polymeric chains (1–10 nm thick) that impede water and ion diffusion towards the copper surface.[8c,9,13] Despite their high efficiency in corrosion inhibition, benzotriazole films suffer from limited thermal stability, and degradation was observed upon exposure of benzotriazole-coated copper films to 100 °C under atmospheric conditions.[9]

The limitations mentioned above have motivated us to develop a different approach for copper protection, which is based on the self-assembly of *N*-heterocyclic carbenes (NHCs). The strong and stable anchoring of NHCs to coinage metals has led to their wide utilization for monolayer formation.[14] It has been demonstrated that NHCs can bind to copper surfaces[15] and that NHCs' deposition led to copper-oxide reduction.[16] However, the limited stability of NHC monolayers under harsh conditions and challenges in their uniform deposition have restricted their applicability for mitigating copper films oxidation. Self-assembly of chemically-addressable NHCs opened a new route for tuning surface properties, such as work function, wettability and chemical nature.[14b,c,17] As demonstrated herein, electro-deposition of alkyne-functionalized NHCs on copper films induced on-surface polymerization for the formation of

[*] I. Berg,[+] E. Amit,[+] Prof. E. Gross
Institute of Chemistry and the Center for Nanoscience and Nanotechnology, The Hebrew University
Jerusalem 91904 (Israel)
E-mail: elad.gross@mail.huji.ac.il

Dr. L. Hale, Prof. F. D. Toste
Department of Chemistry, University of California
Berkeley, CA 94720 (USA)

[+] These authors contributed equally to this work.

NHC-nanolayer that was found effective in mitigating copper oxidation (Scheme 1).

NHC-nanolayer formation on copper film was induced by exposure of alkyne-functionalized imidazolium cation to hydroxide ions that were formed near the copper electrode by electrochemical water reduction.[18] Deprotonation of the imidazolium cation led to the formation and self-assembly of NHCs on copper surface. In addition, the alkyne side groups of the self-assembled NHCs were deprotonated by the hydroxide ions and functioned as an active group for on-surface polymerization between surface-anchored and solvated NHCs, yielding a self-limited 2.0 ± 0.5 nm thick NHC-nanolayer. The NHC-nanolayer effectively hindered copper oxidation while demonstrating high thermal- and chemical-stability under various oxidizing conditions.

Results and Discussion

Alkyne-functionalized imidazolium salt (1,3-di(prop-2-yn-1-yl)-1*H*-imidazolium iodide) was synthesized[19] and electrochemically deposited[18] on copper film. During the electrochemical deposition, hydroxide ions were formed near the copper electrode by applying a negative potential (−1.3 V vs. Ag/Ag^+) that led to water reduction. The hydroxide ions function as a base for deprotonation of imidazolium cations ($pK_a=22$),[20] enabling active carbene formation in proximity to the electrode surface that led to self-assembly of NHC monolayer. In addition to deprotonation of the imidazolium proton, the alkyne groups ($pK_a=25$)[21] of surface-anchored NHCs were deprotonated by the hydroxide ions thus enabling on-surface polymerization between surface-anchored and solvated NHCs, resulting in NHC-nanolayer formation on copper film.

NHC nanolayer was characterized by N 1s X-ray photoelectron spectroscopy (XPS) measurement (Figure 1a, spectrum i). The N 1s XPS spectrum showed a broad peak that was fit by two Gaussians, centered at 398.9 eV and 400.7 eV and assigned to C–N=C and N–C bonds, respectively.[17f] For comparison, dimethyl-benzimidazolium iodide (DMBI) was used as a precursor for monolayer formation on copper film due to its ability to form densely-packed NHC monolayers.[22] The N 1s XPS signal of copper-supported NHC monolayer, prepared by using DMBI as a precursor, was measured (Figure 1a, spectrum ii). The N 1s XPS peak area of the alkyne-NHC was four-fold higher than that of DMBI monolayer. Thus, on average, the alkyne-NHC nanolayer contains four layers of NHCs.

A lamella was extracted from NHC-nanolayer coated copper film using a focused ion beam (FIB) and the nanolayer thickness was assessed by scanning transmission electron microscopy energy dispersive X-ray spectroscopy (STEM-EDS) analysis. A protective iridium layer was deposited on the nanolayer before its extraction in order to prevent beam damage. Cross-sectional STEM-EDS analysis of the extracted lamella (Figure 1b) revealed a 2.0 ± 0.5 nm thick organic layer between the copper film and the protective iridium layer. Since NHC monolayer thickness is ≈0.5 nm,[23] the measured thickness of the NHC nanolayer indicates that it is constructed of four layers of NHC. This result nicely matches the XPS results (Figure 1a) that showed a 4-fold increase in the N 1s XPS peak area of NHC nanolayer in comparison to DMBI monolayer.

The influence of EC-deposition duration on nanolayer thickness was examined by analysis of the N 1s XPS signal as a function of the applied-voltage duration. It was identified that the polymerization rate decreases with the EC-deposition duration (Figure S1). Growth deceleration was attributed to the deteriorated conductivity of copper film coated with an insulating polymer layer (Figure S2), which hinders the formation of hydroxide ions. The growth of an insulating nanolayer was validated by probing the continuous decrease in the current during on-surface polymerization (Figure S3). The influence of water concentration on nanolayer formation was analyzed and a reduction of up to 20% in nanolayer formation yield was probed as water concertation was gradually decreased (Table S1).

Resistivity measurements demonstrated that the presence of NHC nanolayer increased the Cu film resistivity by 6%, in comparison to Cu film that was exposed to the reducing deposition conditions, but without the imidazolium precursor (Table S2). Thus, the surface-anchoring of NHC nanolayer had a relatively minor impact on the bulk electronic properties of Cu.

Spectroscopic measurements were conducted in order to shed light on the molecular properties of NHC-nanolayer and its formation mechanism. Raman spectra of the imidazolium salt precursor revealed a single peak at

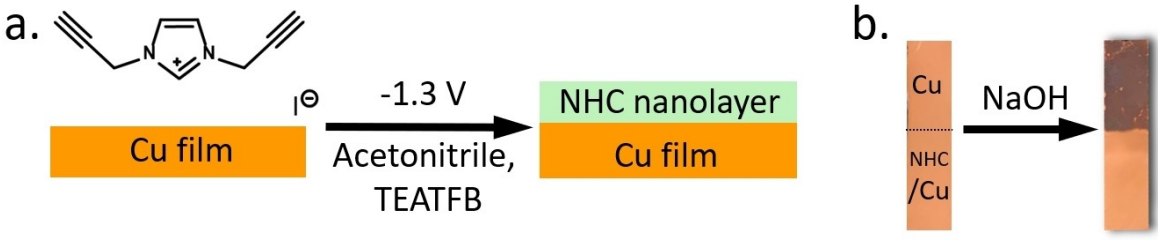

Scheme 1. a) NHC nanolayer was self-assembled on copper film by electrochemically induced deprotonation of alkyne-functionalized imidazolium (Tetraethylammonium tetrafluoroborate = TEATFB). b) Copper film (1×4 cm) was coated in its lower half with NHC nanolayer while the upper half was kept bare. The copper film was then fully immersed in 0.1 M NaOH for 2 h. A photo of the copper film before (left) and after (right) exposure to NaOH shows that the nanolayer-coated copper area (lower half) preserved its metallic color, while the bare copper area (upper half) changed its color due to oxidation.

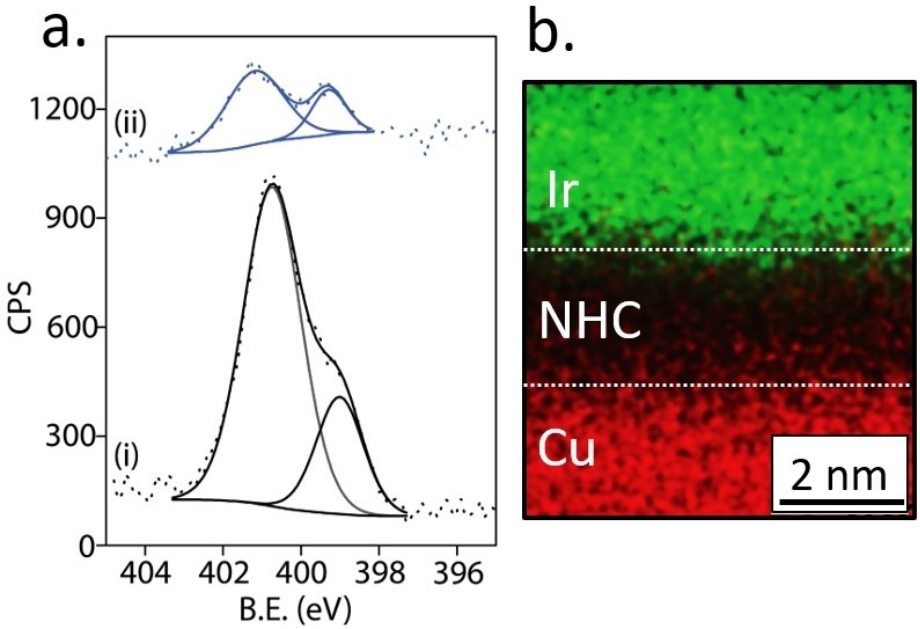

Figure 1. a) N 1s XPS spectrum of NHC-nanolayer (i) and DMBI monolayer (ii) that were electrochemically-deposited on copper film. b) STEM-EDS analysis of a lamella extracted from the NHC-nanolayer coated copper film. Protective iridium film was deposited on the nanolayer before extraction.

1560 cm^{-1} (Figure 2a, spectrum i), correlated to the symmetric stretching vibration of the imidazolium ring.[24] An additional peak was detected at 2130 cm^{-1} (Figure 2b, spectrum i), matching the symmetric C≡C stretching vibration.[25] Attenuated total reflection infrared (ATR-IR) spectra of the imidazolium salt precursor revealed a sharp peak at 3290 cm^{-1}, correlated to the ≡C–H vibration (Figure S4).

Raman spectra of the nanolayer-coated sample showed a broad peak at ≈1600 cm^{-1}, correlated to surface-anchored carbene ring (Figure 2a, spectrum ii).[17c,d] It is hypothesized that the basic environment of the electrochemical deposition induced polymerization of solvated alkyne-NHCs with surface-anchored NHCs under anionic reaction conditions for polyacetylene formation.[26] Polyacetylenes are well known to be susceptible to oxidation[27] and the presence of a carbonyl-related peak at 1780 cm^{-1} (Figure 2a, spectrum ii) indicates that the unsaturated bonds in the nanolayer were oxidized. No peak was detected in the C≡C bond region of the nanolayer-coated copper film (Figure 2b, spectrum ii), indicating that alkyne concentration was diminished following deposition. IR spectrum of the nanolayer showed as-well

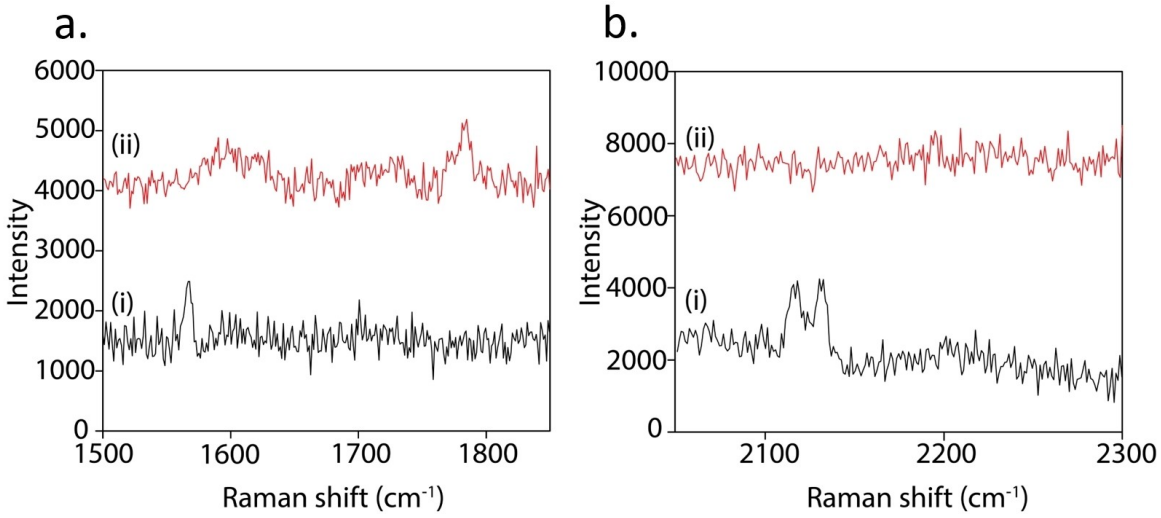

Figure 2. Raman spectra of alkyne-functionalized imidazolium salt (i) and NHC nanolayer (ii) on copper film, in the double bond frequency range (a) and triple bond frequency range (b).

the diminishing of the C≡C vibration amplitude following surface-anchoring along with the presence of various carbonyl-related signatures (Figure S5). The NHC-nanolayer oxidation was also probed in C 1s XPS measurements that showed threefold higher CO_x related features in the nanolayer spectrum in comparison to DMBI monolayer (Figure S6).

NHC polymerization was also induced by exposure of alkyne-functionalized imidazolium salt to a solution of potassium tert-butoxide. However, in contrast to on-surface electro-polymerization, the solution phase polymerization was not self-limited and led to precipitation. ATR-IR spectrum of the precipitated polymer did not identify the strong ≡C–H signal that was detected in the imidazolium precursor (Figure S4). In addition, it was observed that the IR alkene signal in the nanolayer was an order of magnitude higher than that of alkyne (Figure S5). The formation of NHC oligomers with 3–4 repeating units should have led to higher alkyne to alkene signals ratio and should not have fully quenched the ≡C–H signal. The spectroscopic results can therefore indicate that the polymerization process was not restricted to short oligomers formation and can lead to formation of longer chains in solution phase or interconnected oligomers on the Cu surface.

The polymerization mechanism was studied by monitoring the influence of TEMPO ((2,2,6,6-tetramethylpiperidin-1-yl)oxyl), which is a radical scavenger,[28] addition on NHC-nanolayer formation. XPS measurements revealed that TEMPO addition did not influence the nanolayer formation (Figure S7), thus indicating that the polymerization does not involve a radical-based formation mechanism. Electrodeposition of alkyne-NHC in the presence of ascorbic acid, which functions as both acid and radical scavenger,[17g] prevented the polymerization process and exclusively led to NHC monolayer formation, as identified by a 4-fold decrease in the N 1s XPS peak area (Figure S8). This result can be rationalized by the higher pK_a value of the alkyne groups compared to the imidazolium cations, leading to efficient quenching of the alkyne-based polymerization process.[20] Monolayer formation was still achieved even in the presence of ascorbic acid due to the lower pK_a value of the imidazolium cation and the high proximity between deprotonated NHCs and copper surface, which enabled surface anchoring. Nanolayer formation was also quenched once the alkyne group was protected with triisopropylsilyl (TIPS) group.[17g] This result demonstrates the crucial role of alkyne deprotonation in initiating nanolayer formation. Based on the spectroscopic measurements, a hypothesized scheme for on-surface anchoring and polymerization was suggested (Scheme 2).

The oxidation state of nanolayer-coated copper film was detected by XPS and Auger spectra (Figures 3a and b, respectively). Cu2p XPS spectrum of nanolayer-coated copper film showed a dominant peak at 932.7 eV, correlated to Cu^0/Cu^{1+} (Figure 3a, spectrum i). No indication for Cu^{2+} species (≈942.5 eV) was detected on the nanolayer-coated surface.[29] Since Cu^0 and Cu^{1+} cannot be differentiated in XPS measurement, X-ray-induced Auger electron spectroscopy measurements were performed to distinguish between these oxidation states. Auger spectrum of nanolayer-coated copper film (Figure 3b, spectrum i), showed a noticeable peak at 918.5 eV, indicative of the presence of Cu^0 species. Another peak was detected at 916.5 and was correlated to Cu^{1+} species.[16]

The nanolayer-coated copper film was exposed to oxidizing conditions (100 °C, air, 4 h) to assess the functionality of the organic layer for corrosion inhibition. The XPS spectrum of nanolayer-coated copper film did not noticeably change after exposure to oxidizing conditions (Figure 3a, spectrum ii).[30] Changes in the Auger spectrum following exposure to oxidizing conditions indicated that partial oxidation from Cu^0 to Cu^{1+} was induced. However, a

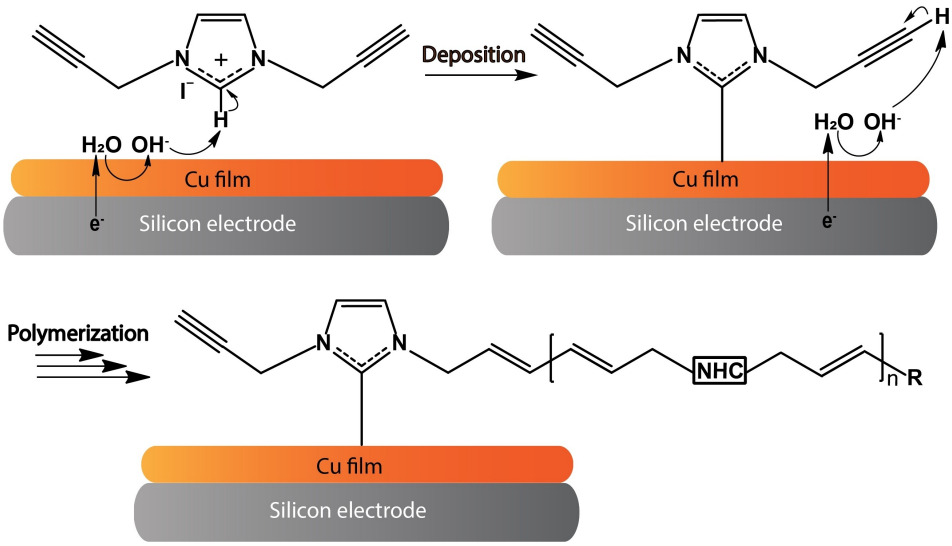

Scheme 2. Hypothesized scheme for on-surface nanolayer formation. For simplicity, polymerization is shown for only one of the two alkyne groups. R = alkyne-functionalized NHC.

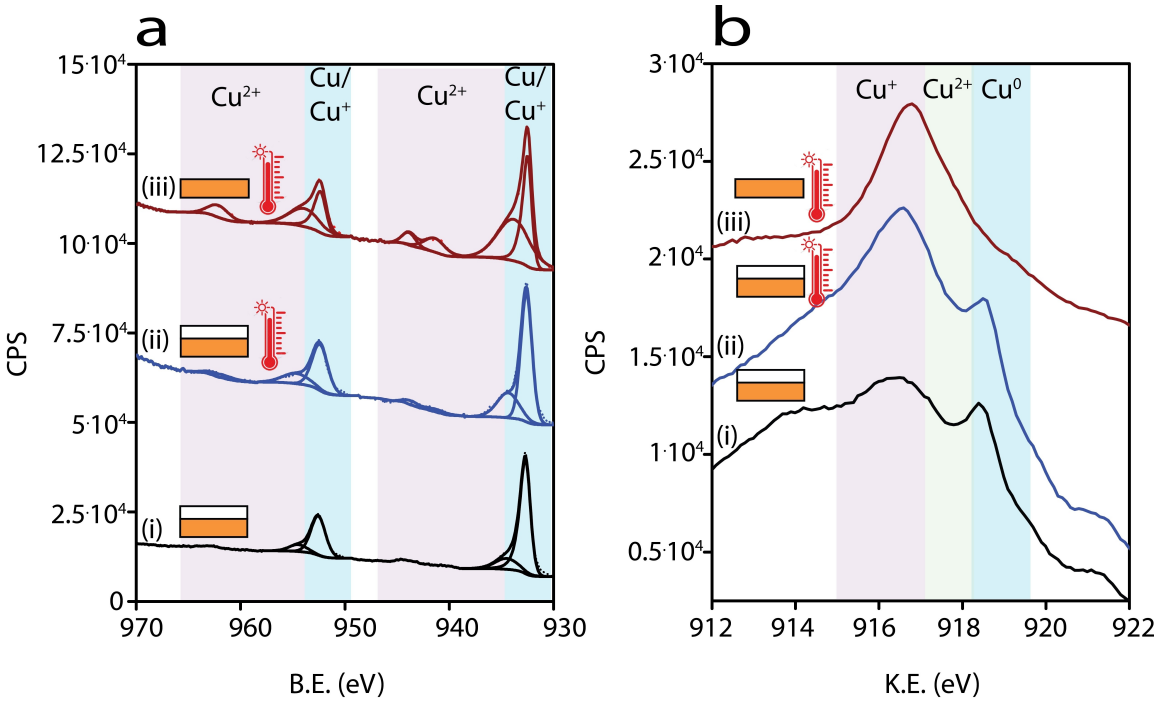

Figure 3. Cu2p XPS spectra (a) and Cu LMM Auger spectra (b) of a nanolayer-coated copper film before (i) and after (ii) exposure to 100 °C for 4 h under air and bare copper surface following exposure to 100 °C for 4 h under air (iii).

dominant Cu^0 peak was still detected and demonstrated that the nanolayer-coated copper surface did not lose its metallic character.

Exposure of a bare copper film to identical oxidizing conditions led to the appearance of a noticeable XPS peak at 942.5 eV, correlated to Cu^{2+} species (Figure 3a, spectrum iii). This peak was not detected prior to exposure of the non-coated copper film to oxidizing conditions (Figure S9). Auger spectra of the bare surface after exposure to oxidizing conditions showed no indication for a peak at ≈918.5 eV, which is indicative of complete oxidation of Cu^0 to Cu^{1+} and Cu^{2+} (Figure 3b, spectrum iii). Longer exposure duration of the nanolayer-coated sample to oxidizing conditions had some influence on copper oxidation (Figure S10). However, exposure of the nanolayer-coated copper film to elevated temperatures (150 and 200 °C) led to noticeable copper oxidation, as indicated by the Cu^{2+} signature appearance in the XPS spectra (Figure S10).

In order to compare the effectiveness of NHC-nanolayer versus NHC-monolayer in mitigating copper oxidation, the properties of DMBI-coated copper film were measured following exposure to oxidizing conditions (100 °C, air, 4 h). The oxidation mitigation functionality of DMBI-coated copper film was inferior in comparison to NHC-nanolayer (Figure S11). Moreover, N 1s XPS measurements of DMBI-coated copper film did not detect any nitrogen signal following exposure to oxidizing conditions, demonstrating its limited stability. It should be noted that in a similar way to DMBI, both benzotriazole and alkanethiols, which have been used as corrosion inhibitors[31] showed inadequate thermal stability with noticeable deformation following exposure to 100 °C under atmospheric conditions.[8b,9]

The nanolayer-coated and bare copper films were exposed to NaOH (0.1 M, 2 h) and then characterized by XPS and Auger measurements (Figure 4a and b, respectively). Exposure to NaOH led to partial surface oxidation as identified by detection of Cu^{2+} peak in the XPS spectra of the nanolayer-coated and bare copper films (spectra i and ii, respectively). The Cu^{2+} peak area (937–947 eV) in the XPS spectrum of the bare copper sample was four-fold higher than that of the nanolayer-coated sample. Auger spectrum of nanolayer-coated copper film showed a peak in the range of Cu^{1+}/ Cu^{2+} and a shoulder at 918.5 eV, which was correlated to Cu^0 species (Figure 4b, spectrum i). Auger spectrum of the bare copper, following its exposure to NaOH, showed a dominant peak at 917.5 eV (correlated to Cu^{2+} species) with no signature at ≈918.5 eV that can be correlated to Cu^0 (Figure 4b, spectrum ii).

Integration of the XPS and Auger data indicates that the bare copper film was fully oxidized to Cu^{2+} and Cu^{1+} with no indication for Cu^0, following exposure to NaOH. The nanolayer-coated Cu film was less oxidized and Cu^0 was still detected after exposure to NaOH. The oxidation mitigation ability of NHC-nanolayer was also observed visually (Scheme 1b) as the nanolayer-coated copper film maintained a metallic copper luster even after exposure to 0.1 M NaOH, while the non-coated copper film was dull, indicative of surface oxidation.

It is postulated that the improved thermal and chemical stability of NHC-nanolayer, in comparison to NHC- and thiol-based monolayers, are linked with the strong metal-

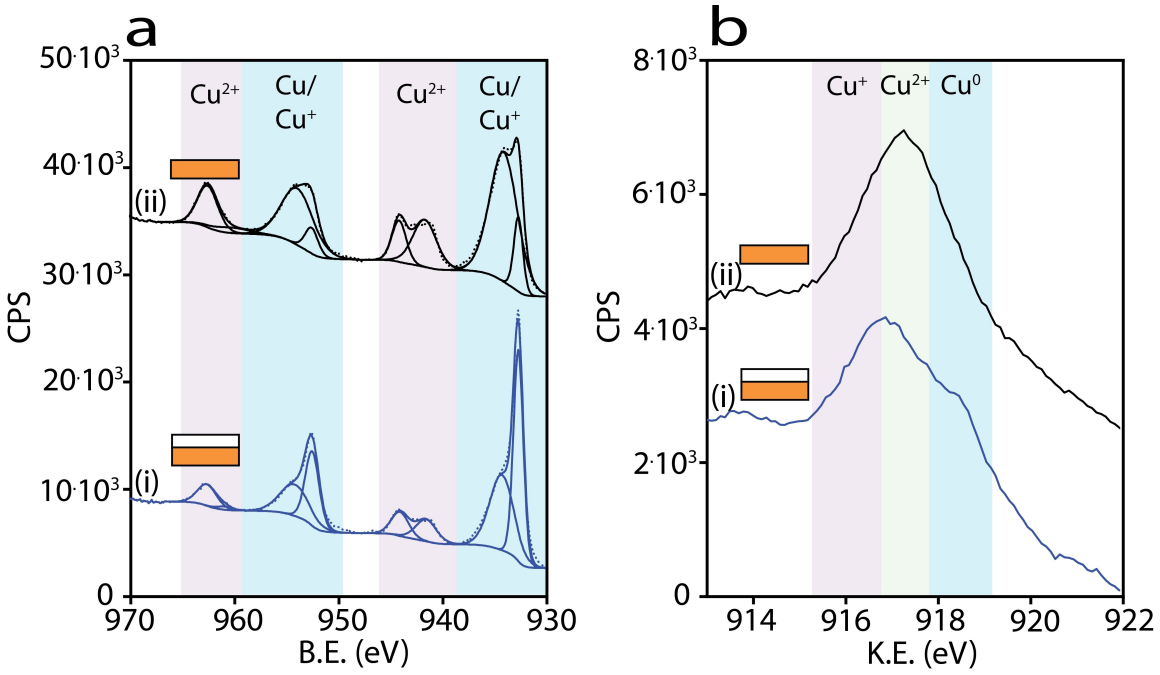

Figure 4. a) Cu2p XPS and b) Cu LMM Auger spectra of (i) nanolayer-coated copper film and (ii) bare copper film following their immersion in 0.1 M NaOH for 2 h.

carbene bond[14f] and the ability to construct interconnections between neighboring NHCs in the encapsulating nanolayer. The encapsulating nature of NHC-nanolayer can be further utilized for coating and protecting rough surfaces, which cannot be easily achieved while using organic monolayers such as benzotriazole, alkanethiols, and formate.[5,8]

The electrodeposition of NHC-nanolayer is comparable to electrografting of aryldiazonium salts,[31b,32] which are surface-anchored and polymerized in a radical process under reducing conditions. However, the radical-based mechanism of aryldiazonium polymerization and the fact that the surface anchoring and polymer forming groups are identical, makes it challenging to control their surface-polymerization process. Our mechanistic study suggests that in alkyne-functionalized NHCs, the carbene group functions as the surface anchoring group while the alkyne group induces the polymerization step. The lower pK_a value of the carbene group compared to the alkyne group, increased the surface-anchoring rate compared to the polymerization step, thus leading to high density of surface-anchored NHCs and preventing a solution-phase polymerization. In addition, the presence of two nitrogen atoms in NHC led to π-electron donation characteristics that further increased the interaction between the NHC and copper surface compared to the aryl-metal interactions.

The presented results show that NHC nanolayer can mitigate Cu film oxidation. It is hypothesized that the functionality of this layer can be further improved by increasing the density of surface anchored molecules and by enhancing the crosslinking between neighboring oligomers toward the formation of a dense nanolayer network. This optimization can be achieved by tuning the chemical structure of alkyne-NHC to enable higher surface density and improved crosslinking capabilities. Exposure of the sample to irradiation can also be utilized for nanolayer network formation, as demonstrated in topochemical polymerization of diacetylenes.[33]

Conclusion

In this work, we demonstrate that a 2 nm thick NHC-nanolayer can be prepared on copper films by using electrochemically assisted deprotonation of alkyne-functionalized imidazolium salt and show that nanolayer-coating provides surface passivation that mitigates copper oxidation. In the electrochemical nanolayer formation process, hydroxide ions are electrochemically formed on a copper electrode by water reduction. The localized base formation enabled deprotonation of the imidazolium salt precursors and NHCs' anchoring on copper electrodes. Alkyne groups were deprotonated by the localized basic environment, leading to on-surface polymerization and nanolayer formation. NHC-nanolayer was characterized by a self-limiting growth mechanism that induced a nanolayer thickness of 2.0 ± 0.5 nm. The high spatial and temporal proximity between the deprotonation, surface-anchoring and polymerization steps enabled the formation of NHC nanolayer on the copper electrode and circumvented the solution-phase polymerization. The pK_a differences between the imidazolium and alkyne groups provided the capability to discriminate between the surface-anchoring and polymerization steps and to form a highly-dense nanolayer, with strong

surface affinity. It is plausible that strong carbene-metal interactions and NHC interconnections in the encapsulating nanolayer provided the high thermal and chemical stability to mitigate copper oxidation in air under elevated temperature (100 °C) and alkaline environment. The oxidation mitigation capabilities of NHC-nanolayer outperformed that of NHC monolayer. The ease of preparation and well-controlled growth process of electrochemically-induced NHC nanolayer make it an easily-applicable method for large-scale coating to provide thin and effective passivation layer for copper surfaces. Moreover, the electro-induced mechanism of NHC-nanolayer formation makes it possible to selectively deposit the protective layer on conducting copper wires without changing the optical properties of the entire device. These advantages make the presented technology highly suitable for applications that require high transparency, such as solar cells and electroluminescence devices.

Acknowledgements

This research was supported by the European Research Council (ERC) under the European Union's Horizon 2020 research and innovation program (Grant Agreement No. 802769, ERC Starting Grant "MapCat"). I.B. thanks the Clore Foundation for the award of Clore Ph.D. Fellowship.

Conflict of Interest

The authors declare no competing financial interest.

Data Availability Statement

The data that support the findings of this study are available from the corresponding author upon reasonable request.

Keywords: N-Heterocyclic Carbenes · Self-Assembled Monolayers · Surface Coating

[1] H. W. Richardson, *Handbook of copper compounds and applications*, Marcel Dekker, New York, **1997**.
[2] S. Magdassi, M. Grouchko, A. Kamyshny, *Materials* **2010**, *3*, 4626–4638.
[3] a) J. Li, J. W. Mayer, E. G. Colgan, *J. Appl. Phys.* **1991**, *70*, 2820–2827; b) P. C. Hsu, H. Wu, T. J. Carney, M. T. McDowell, Y. Yang, E. C. Garnett, M. Li, L. B. Hu, Y. Cui, *ACS Nano* **2012**, *6*, 5150–5156.
[4] C. Gattinoni, A. Michaelides, *Surf. Sci. Rep.* **2015**, *70*, 424–447.
[5] J. Peng, B. L. Chen, Z. C. Wang, J. Guo, B. H. Wu, S. Q. Hao, Q. H. Zhang, L. Gu, Q. Zhou, Z. Liu, S. Q. Hong, S. F. You, A. Fu, Z. F. Shi, H. Xie, D. Y. Cao, C. J. Lin, G. Fu, L. S. Zheng, Y. Jiang, N. F. Zheng, *Nature* **2020**, *586*, 390–394.
[6] a) W. A. Lanford, P. J. Ding, W. Wang, S. Hymes, S. P. Muraka, *Thin Solid Films* **1995**, *241–234*, 262; b) V. V. Nikam, R. G. Reddy, *J. Power Sources* **2005**, *152*, 146–155.
[7] a) S. Hymes, S. P. Murarka, C. Shepard, W. A. Lanford, *J. Appl. Phys.* **1992**, *71*, 4623–4625; b) B. L. Hurley, R. L. McCreery, *J. Electrochem. Soc.* **2003**, *150*, B367–B373; c) A. I. Muñoz, J. G. Anton, J. L. Guinin, V. P. Herranz, *Electrochim. Acta* **2004**, *50*, 957–966; d) F. Mahvash, S. Eissa, T. Bordjiba, A. C. Tavares, T. Szkopek, M. Siaj, *Sci. Rep.* **2017**, *7*, 42139.
[8] a) P. E. Laibinis, G. M. Whitesides, *J. Am. Chem. Soc.* **1992**, *114*, 9022–9028; b) D. A. Hutt, C. Q. Liu, *Appl. Surf. Sci.* **2005**, *252*, 400–411; c) F. Grillo, D. W. Tee, S. M. Francis, H. A. Fruchtl, N. V. Richardson, *J. Phys. Chem. C* **2014**, *118*, 8667–8675.
[9] T. M. Christensen, N. R. Sorensen, *Surf. Interface Anal.* **1991**, *17*, 3–6.
[10] F. Caprioli, F. Decker, A. G. Marrani, M. Beccari, V. Di Castro, *Phys. Chem. Chem. Phys.* **2010**, *12*, 9230–9238.
[11] a) D. Chadwick, T. Hashemi, *Corros. Sci.* **1978**, *18*, 39–51; b) M. Finšgar, I. Milošev, *Corros. Sci.* **2010**, *52*, 2737–2749; c) O. Geuli, D. Mandler, *Corros. Sci.* **2018**, *143*, 329–336.
[12] S. Liu, J. M. Duan, R. Y. Jiang, Z. P. Feng, R. Xiao, *Mater. Corros.* **2011**, *62*, 47–52.
[13] F. M. Al Kharafi, A. M. Abdullah, I. M. Ghayad, B. G. Ateya, *Appl. Surf. Sci.* **2007**, *253*, 8986–8991.
[14] a) K. V. S. Ranganath, J. Kloesges, A. H. Schafer, F. Glorius, *Angew. Chem. Int. Ed.* **2010**, *49*, 7786–7789; *Angew. Chem.* **2010**, *122*, 7952–7956; b) A. V. Zhukhovitskiy, M. G. Mavros, T. Van Voorhis, J. A. Johnson, *J. Am. Chem. Soc.* **2013**, *135*, 7418–7421; c) C. M. Crudden, J. H. Horton, I. I. Ebralidze, O. V. Zenkina, A. B. McLean, B. Drevniok, Z. She, H. B. Kraatz, N. J. Mosey, T. Seki, E. C. Keske, J. D. Leake, A. Rousina-Webb, G. Wu, *Nat. Chem.* **2014**, *6*, 409–414; d) A. V. Zhukhovitskiy, M. J. MacLeod, J. A. Johnson, *Chem. Rev.* **2015**, *115*, 11503–11532; e) C. A. Smith, M. R. Narouz, P. A. Lummis, I. Singh, A. Nazemi, C. H. Li, C. M. Crudden, *Chem. Rev.* **2019**, *119*, 4986–5056; f) M. Koy, P. Bellotti, M. Das, F. Glorius, *Nat. Catal.* **2021**, *4*, 352–363.
[15] a) C. R. Larrea, C. J. Baddeley, M. R. Narouz, N. J. Mosey, J. H. Horton, C. M. Crudden, *ChemPhysChem* **2017**, *18*, 3536–3539; b) L. Jiang, B. D. Zhang, G. Medard, A. P. Seitsonen, F. Haag, F. Allegretti, J. Reichert, B. Kuster, J. V. Barth, A. C. Papageorgiou, *Chem. Sci.* **2017**, *8*, 8301–8308.
[16] A. J. Veinot, A. Al-Rashed, J. D. Padmos, I. Singh, D. S. Lee, M. R. Narouz, P. A. Lummis, C. J. Baddeley, C. M. Crudden, J. H. Horton, *Chem. Eur. J.* **2020**, *26*, 11431–11434.
[17] a) A. F. Lv, M. Freitag, K. M. Chepiga, A. H. Schafer, F. Glorius, L. F. Chi, *Angew. Chem. Int. Ed.* **2018**, *57*, 4792–4796; *Angew. Chem.* **2018**, *130*, 4883–4887; b) S. Dery, S. Kim, G. Tomaschun, I. Berg, D. Feferman, A. Cossaro, A. Verdini, L. Floreano, T. Kluner, F. D. Toste, E. Gross, *J. Phys. Chem. Lett.* **2019**, *10*, 5099–5104; c) S. Dery, S. Kim, G. Tomaschun, D. Haddad, A. Cossaro, A. Verdini, L. Floreano, T. Kluner, F. D. Toste, E. Gross, *Chem. Eur. J.* **2019**, *25*, 15067–15072; d) S. Dery, I. Berg, S. Kim, A. Cossaro, A. Verdini, L. Floreano, F. D. Toste, E. Gross, *Langmuir* **2020**, *36*, 697–703; e) S. Dery, I. Alshanski, E. Mervinetsky, D. Feferman, S. Yitzchaik, M. Hurevich, E. Gross, *Chem. Commun.* **2021**, *57*, 6233–6236; f) S. Dery, P. Bellotti, T. Ben-Tzvi, M. Freitag, T. Shahar, A. Cossaro, A. Verdini, L. Floreano, F. Glorius, E. Gross, *Langmuir* **2021**, *37*, 10029–10035; g) I. Berg, L. Hale, M. Carmiel-Kostan, F. D. Toste, E. Gross, *Chem. Commun.* **2021**, *57*, 5342–5345; h) D. T. Nguyen, M. Freitag, C. Gutheil, K. Sotthewes, B. J. Tyler, M. Bockmann, M. Das, F. Schluter, N. L. Doltsinis, H. F. Arlinghaus, B. J. Ravoo, F. Glorius, *Angew. Chem. Int. Ed.* **2020**, *59*, 13651–13656; *Angew. Chem.* **2020**, *132*, 13754–13759; i) D. T. Nguyen, M. Freitag, M. Korsgen, S. Lamping, A. Ruhling, A. H. Schafer, M. H. Siekman, H. F. Arlinghaus, W. G. van der Wiel, F. Glorius, B. J. Ravoo, *Angew. Chem. Int. Ed.* **2018**, *57*, 11465–11469; *Angew. Chem.* **2018**, *130*, 11637–11641.

[18] E. D. Amit, S. Dery, S. Kim, A. Roy, Q. Hu, V. Gutkin, H. Eisenberg, T. Stein, D. Mandler, F. D. Toste, E. Gross, *Nat. Commun.* **2020**, *11*, 5714–5724.
[19] A. Johnson, M. C. Gimeno, *Organometallics* **2017**, *36*, 1278–1286.
[20] S. Tshepelevitsh, A. Kutt, M. Lokov, I. Kaljurand, J. Saame, A. Heering, P. G. Plieger, R. Vianello, I. Leito, *Eur. J. Org. Chem.* **2019**, 6735–6748.
[21] B. Elvers, G. Bellussi, *Ullmann's encyclopedia of industrial chemistry*, 7th, completely rev. ed., Wiley-VCH, Weinheim, **2011**.
[22] C. M. Crudden, J. H. Horton, M. R. Narouz, Z. J. Li, C. A. Smith, K. Munro, C. J. Baddeley, C. R. Larrea, B. Drevniok, B. Thanabalasingam, A. B. McLean, O. V. Zenkina, I. I. Ebralidze, Z. She, H. B. Kraatz, N. J. Mosey, L. N. Saunders, A. Yagi, *Nat. Commun.* **2016**, *7*, 12654.
[23] G. Q. Wang, A. Ruhling, S. Amirjalayer, M. Knor, J. B. Ernst, C. Richter, H. J. Gao, A. Timmer, H. Y. Gao, N. L. Doltsinis, F. Glorius, H. Fuchs, *Nat. Chem.* **2017**, *9*, 152–156.
[24] J. G. Mesu, T. Visser, F. Soulimani, B. M. Weckhuysen, *Vib. Spectrosc.* **2005**, *39*, 114–125.
[25] H. B. Zhang, G. L. Schrader, *J. Catal.* **1985**, *95*, 325–332.
[26] V. M. Kobryanskii, *J. Polym. Sci. Polym. Chem. Ed.* **1992**, *30*, 1935–1939.
[27] F. G. Will, D. W. Mckee, *J. Polym. Sci. Polym. Chem. Ed.* **1983**, *21*, 3479–3492.
[28] E. Niki, *Am. J. Clin. Nutr.* **1991**, *54*, S1119–S1124.
[29] J. P. Espinós, J. Morales, A. Barranco, A. Caballero, J. P. Holgado, A. R. Gonzalez-Elipe, *J. Phys. Chem. B* **2002**, *106*, 6921–6929.
[30] M. C. Biesinger, *Surf. Interface Anal.* **2017**, *49*, 1325–1334.
[31] a) P. G. Fox, G. Lewis, P. J. Boden, *Corros. Sci.* **1979**, *19*, 457–467; b) M. Ceccato, A. Bousquet, M. Hinge, S. U. Pedersen, K. Daasbjerg, *Chem. Mater.* **2011**, *23*, 1551–1557.
[32] a) J. Pinson, F. Podvorica, *Chem. Soc. Rev.* **2005**, *34*, 429–439; b) C. Combellas, F. Kanoufi, J. Pinson, F. I. Podvorica, *J. Am. Chem. Soc.* **2008**, *130*, 8576–8577.
[33] J. Deschamps, M. Balog, B. Boury, M. Ben Yahia, J. S. Filhol, A. van der Lee, A. Al Choueiry, T. Barisien, L. Legrand, M. Schott, S. G. Dutremez, *Chem. Mater.* **2010**, *22*, 3961–3982.

Manuscript received: January 20, 2022
Accepted manuscript online: March 21, 2022
Version of record online: April 6, 2022

Please note: Minor changes have been made to this manuscript since its publication in Angewandte Chemie Early View. The Editor.